Journal of Experimental Botany, Vol. 57, No. 15, pp. 4171–4187, 2006
doi:10.1093/jxb/erl194 Advance Access publication 16 November, 2006

Journal of Experimental Botany

RESEARCH PAPER

Loss of ovule identity induced by overexpression of the fertilization-related kinase 2 (ScFRK2), a MAPKKK from *Solanum chacoense*

Madoka Gray-Mitsumune[1,*], Martin O'Brien[1,*], Charles Bertrand[2], Faiza Tebbji[1], André Nantel[3] and Daniel P. Matton[1,†]

[1] *Institut de recherche en biologie végétale, Département de sciences biologiques, Université de Montréal, 4101 rue Sherbrooke est, Montréal, Québec, Canada H1X 2B2*

[2] *Département d'Anatomie-Biologie Cellulaire, Université de Sherbrooke, 3001 12ème Avenue Nord, Sherbrooke, QC, Canada J1H 5N4*

[3] *Biotechnology Research Institute, National Research Council, 6100 Royalmount Avenue, Montréal, QC, Canada H4P 2R2*

Received 7 July 2006; Accepted 8 September 2006

Abstract

In order to gain information about protein kinases acting during plant fertilization and embryogenesis, a reverse genetic approach was used to determine the role of protein kinases expressed in reproductive tissues. Two cDNA clones named *ScFRK1* and *ScFRK2* (*Solanum chacoense* fertilization-related kinase 1 and 2) were isolated from an expressed sequence tag (EST) library normalized for weakly expressed genes in fertilized ovaries. These showed significant sequence similarities to members of the mitogen-activated protein kinase kinase kinase (MAPKKK) family. RNA gel blot and RNA *in situ* hybridization analyses confirmed the strong up-regulation of *ScFRK2* in ovules after fertilization. In addition, *ScFRK2* mRNAs accumulate during early ovule development in the megasporocyte and in the integument of developing ovules. Overexpression of *ScFRK2* led to the production of fruits with a severely reduced number of seeds. The seeds that were produced also exhibited developmental retardation. Analysis of ovaries prior to fertilization showed that the seedless phenotype was caused by a homeotic conversion of ovules into carpel-like structures. The present observations are consistent with the role of *ScFRK2* in pre- and post-fertilization events. Furthermore, overexpression of *ScFRK2* led to changes in the expression of the class D floral homeotic gene *ScFBP11*, suggesting that the ScFRK2 kinase may interact, directly or indirectly, with the FBP7/11 pathway that directs establishment of ovule identity.

Key words: Carpel, fruit development, MAPKKK, ovule development, Solanaceae.

Introduction

The pivotal role played by protein phosphorylation in eukaryotic signal transduction is well illustrated by the wide range of phosphorylation cascades that involve mitogen-activated protein kinases (MAPKs) (Treisman, 1996; Robinson and Cobb, 1997). In vertebrates, MAPKs are typically activated in response to various mitotic agents such as hormones and growth factors (Piwien-Pilipuk *et al*., 2002). They have been shown to play an important role in the regulation of cell division and differentiation. The activation of MAPKs occurs by phosphorylation of conserved threonine and tyrosine residues in the activation loop between the catalytic subdomains VII and VIII.

* These authors contributed equally to this work.
† To whom correspondence should be addressed. E-mail: dp.matton@umontreal.ca
GenBank accession numbers: *ScFRK1*, AY427828; *ScFRK2*, AY427829; *ScFBP11*, DN980993.
Abbreviations: CaMV, cauliflower mosaic virus; CS, carpelloid structure; DAP, days after pollination; EST, expressed sequence tag; FRK, fertilization-related kinase; MAPK, mitogen-activated protein kinase; MAPKK, mitogen-activated protein kinase kinase; MAPKKK, mitogen-activated protein kinase kinase kinase; RLK, receptor-like kinase; SEM, scanning electron microscopy; WT, wild type.

This phosphorylation step is produced by dual specificity MAPK kinases (MAPKKs). These MAPKKs are themselves activated on serine and/or threonine by serine/threonine MAPKK kinase (MAPKKK) (Nishihama *et al*., 1995; Madhani and Fink, 1998). In non-plants, the activation of MAPKKKs occurs either through phosphorylation by MAPKKK kinase (MAPKKKK) (Elion, 2000; Sells *et al*., 1997), by the receiver domain of a two-component histidine kinase module (Posas and Saito, 1997), or commonly by G proteins (Fanger *et al*., 1997) and G protein-coupled receptors (Sugden and Clerk, 1997). Cell signals are thus transmitted through a chain of phosphorylation events. In plants, direct modulators of MAPKKK are as yet unknown, and complete cascade modules are only just starting to unfold (Asai *et al*., 2002).

The vast majority of plant developmental mutants described so far have been found to be impaired in the expression of transcription factors, many from the MADS-box family (Jack, 2001). Only a few mutants affecting plant development have been described as encoding protein kinases, although it would be reasonable to assume that post-translational modifications through phosphorylation of a protein involved in a key developmental pathway could be an important regulatory step for its intrinsic activity. Disruption of the signalling cascade would thus also lead to developmental defects. Among the protein kinases known to affect key developmental aspects of plant growth and development, most belong to the receptor-like kinase (RLK) family (Becraft, 2002). Some have also been shown to affect reproductive development. These include the *Clavata 1* RLK gene involved in the regulation of meristem size and maintenance (Clark *et al*., 1993); the *BRI1* RLK involved in brassinosteroid perception (Li and Chory, 1997); the *Petunia PRK1* RLK involved in pollen and embryo sac development (Lee *et al*., 1996, 1997); the extra sporogenous cells (*EXS*) RLK which regulates male germ line cell number, tapetal identity, as well as promoting seed development (Canales *et al*., 2002); the maize *CRINKLY4* (*CR4*) RLK involved in aleurone cell fate (Becraft and Asuncion-Crabb, 2000); the *Arabidopsis CRINKLY4* (*ACR4*), required for proper embryogenesis (Tanaka *et al*., 2002) and involved in cell layer organization during ovule integument and sepal margin development (Gifford *et al*., 2003); the somatic embryogenesis receptor-like kinase (*SERK1*) involved in somatic embryogenesis (Schmidt *et al*., 1997), and expressed in developing ovules and embryo (Hecht *et al*., 2001); and the *Strubbelig* RLK that affects outer integument formation and organ shape although is does not encode a functional kinase domain (Chevalier *et al*., 2005). Although downstream kinase modules transducing the initial signal from these RLKs could be expected, like MAPK transducing modules, none has yet been characterized in development, and only a few MAPK family members have been shown to be involved in developmental processes (Hirt, 2000). Recently, a mutation in the *Arabidopsis thaliana YODA* (*YDA*) gene, which codes for a MAPKKK, has been shown to cause an early embryonic defect (Bergmann *et al*., 2004; Lukowitz *et al*., 2004). In this mutant, the zygote does not elongate properly and the suspensor cells are fused to the embryo. Mutant *yda* seedlings that can make it through maturity show overproduction and crowding of stomata cells (Bergmann *et al*., 2004), reminiscent of the receptor kinase *two many mouths* (*tmm*) mutant phenotype (Nadeau and Sack, 2002). This hints at the presence of a MAPK module involved in embryo development and stomatal distribution. Most MAPK cascades described so far have been implicated early in stress and disease responses (Asai *et al*., 2002; Hirt, 2000; Romeis, 2001; Zhang and Klessig, 2001), and hormone perception (Kieber *et al*., 1993).

In this study, the isolation and functional characterization of a new MAPKKK from the MEKK subfamily in *S. chacoense* is described. Overexpression of this protein kinase, named ScFRK2, affects ovule identity and suggests an involvement in seed and fruit development.

Materials and methods

Plant material

The diploid and self-incompatible wild potato *Solanum chacoense* Bitt. ($2n=2x=24$) was grown in a greenhouse with 14–16 h of light per day. The genotypes used were V22 (S alleles S_{11} and S_{13}) as pollen donor and G4 (S alleles S_{12} and S_{14}) as female progenitor. Plants were hand pollinated. Transgenic lines were generated in the G4 background.

DNA and RNA gel blot analysis

Total RNA was isolated as described previously (Jones *et al*., 1985) or with the Plant RNeasy RNA extraction kit from Qiagen (Mississauga, ON, Canada). The RNA concentration was determined by measuring its absorbance at 260 nm. Concentration and RNA quality were verified on an agarose gel with ethidium bromide staining, and RNA concentration adjustment was done if needed. For each tissue tested, 10 μg of total RNA was separated on a formaldehyde/MOPS gel. RNA was then blotted on Hybond N^+ membranes (GE Healthcare, Baie d'Urfée, QC, Canada), and were UV cross-linked with a Hoefer UV cross-linker (120 mJ cm^{-2}). To confirm equal loading between RNA samples, a 1 kb fragment of *S. chacoense* 18S RNA was PCR amplified and used as a control probe. Prehybridization was performed at 45 °C for 3 h in 50% formamide solution (50% deionized formamide, 6× SCC, 5× Denhardt's solution, 0.5% SDS, and 200 μg ml^{-1} of denatured salmon DNA). Hybridization of the membranes was performed overnight at 45 °C in 50% formamide solution. Genomic DNA isolation was performed with the Plant DNeasy kit from Qiagen. Complete digestion of DNA (10 μg) was carried out overnight with 10 U of restriction enzymes as recommended by the supplier (New England Biolab, Beverly, MA, USA). DNA gel blot analysis was performed as previously described (Sambrook *et al*., 1989) and DNA was transferred to Hybond N^+ membranes prior to cross-linking. Prehybridization was performed for 3 h at 65 °C in 50% phosphate solution [50% of 0.5 M Na_2HPO_4 pH 8.0, 1% bovine serum albumin (BSA), 7% SDS, and 1 mM EDTA], while hybridization was performed overnight under the same conditions used for prehybridization. Probes for the RNA and DNA

gel blot analysis were synthesized by random labelling using the Strip-EZ DNA labelling kit (Ambion, Austin, TX, USA) in the presence of [α-^{32}P]dATP (ICN Biochemicals, Irvine, CA, USA). Following hybridization, membranes were washed for 30 min at 25 °C and 30 min at 35 °C in 2× SSC/0.1% SDS; 30 min at 45 °C and 30 min at 55 °C in 1× SSC/0.1% SDS; and for 10 min at 55 °C in 0.1× SSC/0.1% SDS. Prior to control hybridization with the 18S probe, the membranes were stripped as recommended by the manufacturer (Ambion, Austin, TX, USA), and post-hybridization washes were done twice at 60 °C for 30 min in 0.1× SSC/0.1% SDS. Autoradiography was performed at −86 °C on Kodak Biomax MR film (Interscience, Markham, ON, Canada).

Sequence analysis and phylogeny

The catalytic kinase domain structure of ScFRK2 was defined following the 12 kinase subdomains assignation described previously (Hanks and Hunter, 1995). Protein secondary structure prediction needed for the ScFRK2 subdomain designation was performed with these four prediction tools: JUFO (http://www.jens-meiler.de/jufo.html), PORTER (http://distill.ucd.ie/porter/), PSIpred (http://bioinf.cs.ucl.ac.uk/psipred/), and SCRATCH (http://www.igb.uci.edu/tools/scratch/). Designations of subdomain boundaries were obtained from a consensus of all prediction tools and conserved amino acids specific to each domain. The phylogenetic analysis was accomplished with the trimmed catalytic kinase domain only. Alignment of the protein sequences was performed using ClustalX employing default parameters (Thompson *et al*., 1997). The phylogeny was reconstructed in SplitsTree4 (Huson and Bryant, 2006) using the Neighbor–Joining algorithm (Saitou and Nei, 1987) both from uncorrected distances and from distances corrected using a WAG+Γ+F model (Whelan and Goldman, 2001). The phylogenies were validated using the non-parametric bootstrap with 1000 replicates.

Plant transformation

The *ScFRK2* cDNA was PCR amplified with Pwo polymerase (Roche Diagnostic, Laval, QC, Canada) with *Kpn*I overhang primers. Primers used were FRK2Kpn1, 5′-GGGGTACCGCGGTCGGCG-CAATCTT-3′; and FRK2Kpn2, 5′-GGGGTACCACTTCCAT-CAGGCTTTG-3′. The PCR product was cleaved with *Kpn*I and inserted in a modified pBin19 transformation vector (Bussière *et al*., 2003) with a double enhancer cauliflower mosaic virus (CaMV) 35S promoter. Sense and antisense constructs were determined by plasmid digestion with *Eco*RI, which gives an asymmetric fragmentation according to the orientation of cloned PCR products. Sense and antisense constructs were individually transformed in *Agrobacterium tumefaciens* LBA4404 by electroporation. *Solanum chacoense* plants were transformed by the leaf disc method as previously described (Matton *et al*., 1997).

Tissue fixation and scanning electron microscopy (SEM) observations

Dissected ovaries were fixed in 4% glutaraldehyde for 4 h at room temperature in 0.1 M phosphate buffer ($NaHPO_4$, pH 7.0). After two rinsing steps in 0.1 M phosphate buffer, the tissues were dehydrated in an increasing ethanol series (from 30% to 100%) and critical-point-dried with CO_2, coated with gold–palladium, and viewed in a JEOL JSM-35 SEM.

Tissue fixation and optical microscopy observations

Pistils were fixed in FAA for 24 h at 4 °C (50% ethanol, 1.35% formaldehyde, and 5% glacial acetic acid). Samples were then dehydrated in an increasing series of tert-butyl alcohol (from 70% to pure tert-butyl alcohol). Pistils were infiltrated with Paraplast Plus (Tyco Healthcare Group LP, Mansfield, MA, USA) at 60 °C. Thin sections (10 μm) were prepared from embedded samples, and tissue sections were stained in 0.5% Astra Blue and 1% safranin after removal of paraffin. Alternatively, thin sections (10 μm) were prepared from embedded samples and tissue sections were stained in 0.05% toluidine blue O (Fig. 4V–Y). *In situ* hybridizations were performed as described previously (O'Brien *et al*., 2005). Microscopic observations were taken on a Leica OrthoPlan microscope and pictures were taken with a Leica DFC320 camera.

RNA extraction, probe preparation, cDNA array hybridization, and data analysis

DNA microarrays were printed on UltraGAPS™ Slides (Corning) from 7741 expressed sequence tags (ESTs) corresponding to 6374 unigenes derived from fertilized ovary cDNA libraries covering embryo development from zygote to late torpedo stages in *S. chacoense* (Germain *et al*., 2005). This microarray was used to analyse gene expression profiles in ovaries prior to fertilization in wild-type (WT) and *ScFRK2* mutant plants. Total RNA was extracted from unfertilized WT and *ScFRK2* mutant ovaries using TRIzol® reagent (Invitrogen) according to the manufacturer's instructions. RNA yield and purity were assessed by absorbance determination at both 260 and 280 nm. RNA was only used when the Abs260 nm/Abs280 nm ratio was >1.7. RNA integrity was determined with the RNA 6000 Nano Assay Kit and the Agilent 2100 Bioanalyzer. A 30 μg aliquot of total RNA from WT ovaries was hybridized to microarrays along with the same amount of RNA from *ScFRK2* mutant ovaries for 16 h at 42 °C. Each of the four pools of RNA from WT and *ScFRK2*-OX ovaries was compared with the control RNA in individual microarray hybridizations. Two hybridizations used a Cy3/Cy5 comparison, while the other two used a Cy5/Cy3 ratio. This strategy allowed profiling data to be obtained from four biological replicates whilst simultaneously negating any potential bias that could arise from the choice of labelling dyes. Labelling was performed with cyanine 3-dCTP or cyanine 5-dCTP (1 mM; NEN Life Science, Boston MA, catalogue nos NEL576 and 577). Hybridization and washing were performed as described in the CyScribe Post labeling Kit (Amersham Biosciences) in the CMTTM hybridization chamber (Corning). The DNA microarray slides were scanned with a ScanArray Lite scanner (Perkin Elmer-Cetus, Wellesley, CA; version 2.0) at 10 μm resolution. The resulting 16-bit TIFF files were quantified with QuantArray software (Perkin Elmer-Cetus; versions 2.0 and 3.0). Normalization was performed with Lowess (locally weighted scatter plot smoothing). Statistical analysis and visualization were performed with GeneSpring software (Silicon Genetics, Redwood City, CA, USA) using the available statistical tools (Student's *t*-test of replicate samples showing a variation different from 1).

Results

Isolation and sequence analysis of the ScFRK1 and ScFRK2 kinases

Using a negative selection screen targeting only weakly expressed genes expressed during fertilization and early embryogenesis, 16 different protein kinase clones have been isolated from the MAPK family in *S. chacoense*, a self-incompatible wild potato species close to potato and tomato (Germain *et al*., 2005). Two of these, named *ScFRK1* and *ScFRK2*, were further investigated for their

possible role in fertilization and embryogenesis. Both clones showed strong sequence similarity to the catalytic domain of various MAPKKKs, but lacked a large regulatory domain characteristic of most of these MAPKKKs (Tu *et al*., 1997; Wu *et al*., 1999).

The *ScFRK1* kinase clone (accession no. AY427828) is 1539 bp long [excluding the poly(A) tail] and is likely to represent the full-length *ScFRK1* mRNA since the size of this cDNA corresponds to the size of the mRNA as determined from RNA gel blot analyses (~1.5 kb, data not shown). It codes for an open reading frame of 320 amino acids with an estimated mol. wt. of 36.2 kDa. A stop codon is found upstream and in-frame with the first AUG initiation codon, indicating that the coding region is complete. The longest *ScFRK2* cDNA isolated (accession no. AY427829) consists of 1115 bp [excluding the poly(A) tail] and codes for a predicted 304 amino acid protein with an estimated mol. wt. of 34.3 kDa. A stop codon is also found upstream and in-frame with the first AUG initiation codon, indicating that the coding region is also complete. Both proteins are composed of a catalytic domain that constitutes the major part of the protein (Fig. 1A). The kinase domain starts after the first 10 (for ScFRK1) and five (for ScFRK2) amino acids, and stops 42 (for ScFRK1) and 47 (for ScFRK2) amino acids before the end of the protein, leaving ~50 amino acids for putative regulatory domains.

The ScFRK2 deduced protein showed the strongest amino acid sequence identity with ScFRK1 (45% identity; 60% overall similarity), and with a predicted protein kinase from *A. thaliana* (At5g67080, renamed MAPKKK19), with 36% identity (51% overall similarity) (Fig. 1A). The ScFRK1 deduced protein showed the greatest sequence identity (39%; 50% similarity) with the At3g50310 protein sequence (renamed MAPKKK20), a putative protein kinase from *A. thaliana*. Since initial BLAST comparisons retrieved mostly protein kinases defined as MAPKKKs, and since ScFRK1, ScFRK2, and their most similar *A. thaliana* putative orthologues were considerably smaller than most typical MAPKKKs, lacking a large N- or C-terminal regulatory domain, a phylogenetic analysis was performed with representatives from the MAPK (as the outgroup), MAPKK, MAPKKK, and MAPKKKK families, in order to determine to which family of MAPKs ScFRK1 and ScFRK2 belonged. The phylogenetic analysis was achieved after aligning trimmed kinase domains based on previous sequence alignments and secondary structure predictions (Hanks and Quinn, 1991). Protein kinases from *A. thaliana* previously classified into these various MAPK families were used for the analysis. Two members of the MAPK family were chosen (outgroup), as well as 10 MAPKKs, 80 MAPKKKs (48 from the RAF subfamily, 21 from the MEKK subfamily, and 11 from the ZIK subfamily), and six MAPKKKKs. To simplify the display, and since the ScFRK1 and ScFRK2 kinases were closest to the MEKK, a phylogenetic tree obtained with only the MEKK subfamily from the MAPKKK family is shown in Fig. 1B. Only the tree obtained from uncorrected distances is shown, but the use of corrected distances resulted in a tree with an identical topology (data not shown). This analysis clearly showed that both ScFRK1 and ScFRK2 are members of the MEKK subfamily of the MAPKKKs.

The genomic organization of *ScFRK2* was assayed by PCR amplification on genomic DNA and by restriction enzyme digestion of genomic DNA followed by DNA gel blot analyses. PCR amplification was achieved with primers that amplified the complete *ScFRK2* cDNA clone, including all available 5′ and 3′ untranslated region sequences. Genomic DNA and plasmid PCR amplifications were run side by side on an agarose gel, and no differences in the length of the PCR products could be detected (data not shown), indicating the absence of an intron in the region defined by the primers used. In *A. thaliana*, At5g67080 (MAPKKK19), At3g50310 (MAPKKK20), and At4g36950 (MAPKKK21) are also intronless. DNA gel blot analyses of genomic DNA restriction fragments revealed a simple multibanding pattern for *ScFRK2* hybridization (Fig. 2A). The *Eco*RI and *Nco*I digestions showed three bands, while the *Bam*HI and *Xba*I digestions showed two bands. Since *Eco*RI and *Bam*HI cleave the *ScFRK2* cDNA once, and *Nco*I and *Xba*I do not cleave the *ScFRK2* cDNA, these results suggest that, in *S. chacoense*, the *ScFRK2* gene is present possibly in two to three copies if one of the *Bam*HI fragments contains two copies of *ScFRK2* in tandem.

Fertilization induces ScFRK2 *mRNA accumulation in ovules*

The *ScFRK2* expression pattern was determined by RNA gel blot analysis (Fig. 2B) with various vegetative (stems and leaves), generative (petals), and reproductive tissues (stamens, pollen, pollen tubes, fertilized ovules, styles, and ovaries). Prior to fertilization, the strongest *ScFRK2* mRNA accumulation is observed in stamens and styles, although a basal level of mRNA can be detected in most tissues examined, including roots or tubers (Fig. 2B, and data not shown). Fertilization had a dramatic effect on *ScFRK2* accumulation only in ovaries, as can be seen 2 d after pollination (DAP), and corresponding to ~12 h after fertilization (Fig. 2B). Intriguingly, hybridization with the *ScFRK2* probe detected two transcripts, although not consistently in all experiments (for example, see Fig. 3A). The smaller transcript is estimated at 1.1 kb and corresponds to the expected size for the *ScFRK2* cDNA (1.11 kb). The larger 1.6 kb *ScFRK2* transcript is slightly less abundant in all tissues tested except stamens. Since previous results suggest that the gene has no introns, the present finding suggests that the longer transcript is most probably not a splice variant. Nonetheless, since *ScFRK2* is part of a small gene family, this prompted an attempt to isolate a cDNA corresponding to the longer 1.6 kb

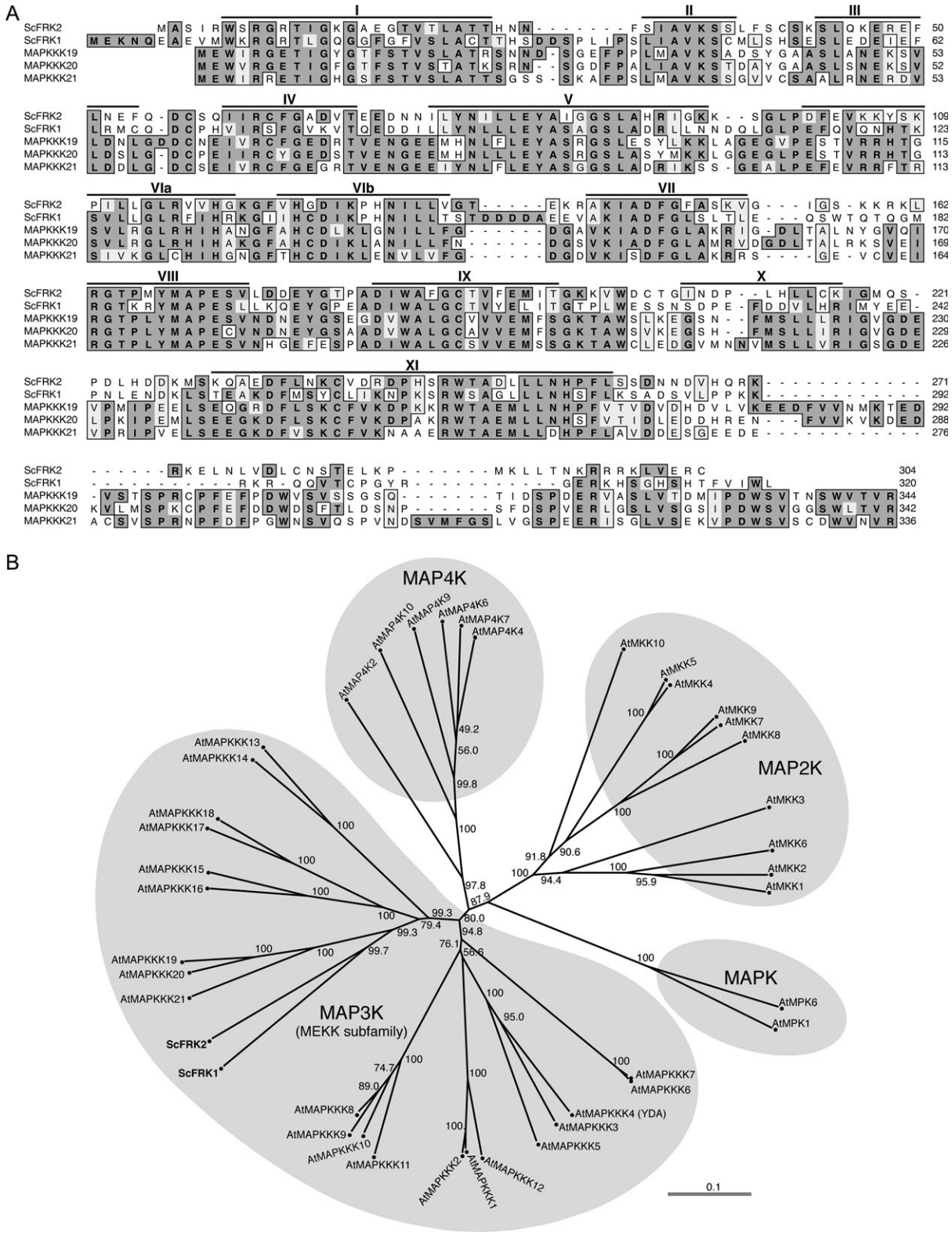

Fig. 1. Sequence analyses of ScFRK1 and ScFRK2. (A) Sequence alignment of the deduced protein sequences from *S. chacoense* ScFRK1 and ScFRK2, and with the three most similar MAPKKKs from *A. thaliana*. Kinase subdomains are identified with thick black lines and were defined as described by Hanks and Hunter (1995), where α-helices and β-sheets were deduced by four different prediction tools (see Materials and methods). (B) Phylogenetic tree obtained with the Neighbor–Joining method from uncorrected distances. Bootstrap support values from 1000 replicates are indicated beside the branches. All *A. thaliana* sequences were directly obtained from the TAIR website (http://www.arabidopsis.org/). The phylogenic analysis was performed using the catalytic kinase domain. Tree branch length is proportional to the number of substitutions, and the scale bar represents the expected number of substitution per site.

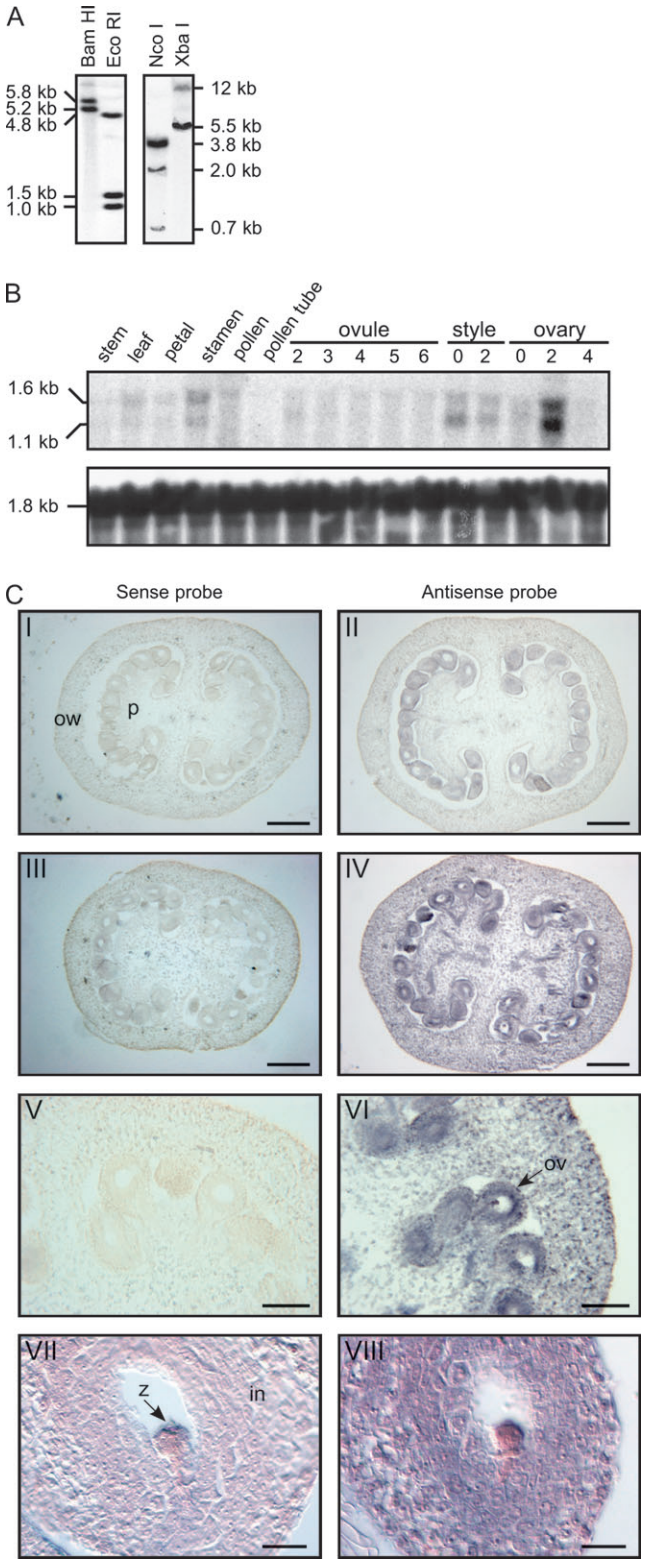

Fig. 2. Transcript profile of *ScFRK2*. (A) DNA gel blot analysis of the *ScFRK2* gene. Genomic DNA (10 μg) isolated from *S. chacoense* leaves was digested with *Bam*HI, *Eco*RI, *Nco*I, or *Xba*I restriction enzymes, transferred onto membranes and probed with the complete 1.1 kb *ScFRK2* cDNA. Estimated molecular weights of the fragments obtained appear on the left of each DNA blot. (B) RNA gel blot analysis of the *ScFRK2* gene. All tissues were collected from greenhouse-grown plants. Pollen tubes were germinated *in vitro*. Fertilized ovules were dissected from ovaries 2–6 d after pollination (DAP). Pistils at 2–4 DAP were separated into styles and ovaries. A 10 mg aliquot of total RNA isolated from *S. chacoense* tissues was blotted and probed using the full-length *ScFRK2* cDNA (upper panel). Membranes were stripped and re-probed using a partial 18S rRNA to ensure equal loading of each RNA sample (lower panel). (C) *In situ* localization of *ScFRK2* transcripts in mature ovaries. I and II, unfertilized mature ovary sections. III and IV, ovary sections 2 DAP (~12 h post-fertilization). V and VI, magnifications of III and IV, respectively. VII and VIII, magnifications of ovary sections 2 DAP showing staining in the zygote. I, III, V, and VII, control sense probe. II, IV, VI, and VIII, antisense sense probe. Digoxigenin labelling is visible as red to purple staining. All hybridizations used 10 μm thick sections and an equal amount of either *ScFRK2* sense or antisense probe. Scale bars, 250 μm (I–IV); 125 μm (V and VI); 20 μm (VII and VIII). In, integument; ov, ovule; ow, ovary wall (pericarp); p, placenta; zy, zygote.

transcript. One million phages from a cDNA library made from 2 DAP pistils were screened using the full-length *ScFRK2* cDNA as a probe. All eight clones that were retrieved corresponded to the 1.1 kb transcript (data not shown). Thus the *ScFRK2* mRNA abundance can be estimated at 0.0008% of total mRNAs in pistil tissues. This is reflected in the exposure time of the hybridization membranes, with 4 d exposure with the *ScFRK2* probe versus 5 min for the control 18S rRNA probe. A 5′ rapid amplifcation of cDNA ends (RACE) PCR was also attempted, but again no product longer than the original *ScFRK2* cDNA could be isolated. Since it is unlikely that the larger *ScFRK2* hybridizing transcript corresponds to an unspliced *ScFRK2* pre-mRNA from the above-mentioned results, the higher molecular weight band may correspond to a cross-hybridizing member of the *ScFRK2* family (Fig. 2A). Alternatively, it cannot be excluded that there is a possibility of an alternative transcription termination site that would generate a longer transcript, although again this species should have been found in the library re-screening.

In order to determine the spatial expression pattern of the *ScFRK2* gene, *in situ* RNA hybridizations were performed using ovaries taken before and after fertilization (Fig. 2C). Before fertilization, a weak *ScFRK2* mRNA signal was detected only in mature ovules (Fig. 2CII). After fertilization, much stronger *ScFRK2* mRNA signals were detected in ovules and, also, diffuse signals were detected in the placenta and ovary wall (Fig. 2CIV and VI). Although preservation and observation of the zygote is difficult in these paraffin-embedded sections, staining can occasionally be observed in the embryo sac where the zygote would be located (e.g. see magnification in Fig. 2CVIII). The absence of or very weak sense probe hybridization signals confirmed the specificity of the detection pattern obtained (Fig. 2CI, III, V, and VII).

ScFRK2 *overexpression lines have defects in ovule development*

Transgenic plants were generated carrying the sense or antisense construct of *ScFRK2*. The *ScFRK2* cDNA was placed downstream of a double enhancer 35S promoter in

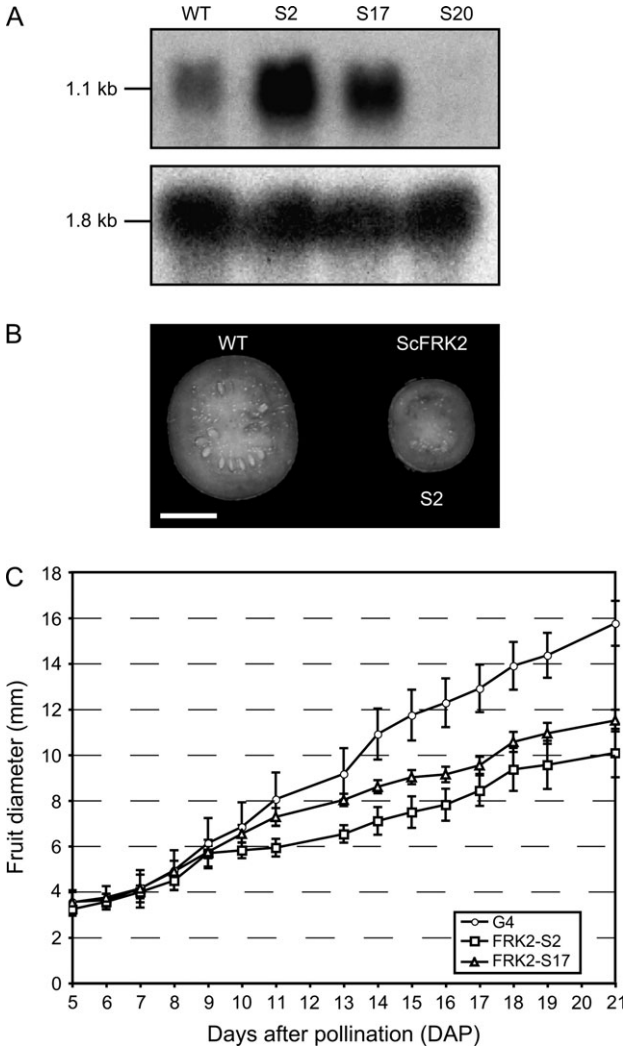

Fig. 3. Analyses of *ScFRK2* transgenic plants carrying sense constructs. (A) RNA gel blot analyses of *ScFRK2* mRNA (upper panel) and 18S rRNA (lower panel) of ovary tissues derived from wild-type plants (WT), overexpression lines S2 and S17, and co-suppression line S20. (B) Comparison of fruit slices. Scale bar, 1 cm. (C) Growth in fruit size after pollination.

a modified pBin19 vector in a sense or antisense orientation (Bussière *et al*., 2003). Kanamycin-resistant plants were grown to maturity in the greenhouse, and the *ScFRK2* expression level was monitored by RNA gel blot analyses of stamen, leaf, and ovary tissues. Identical results were obtained for the three tissues tested, indicating that the CaMV 35S promoter used was equally active in ovaries, stamens, and leaves. Among 13 transgenic lines containing the sense construct, one showed complete co-suppression for *ScFRK2* (line S20 in Fig. 3A), while 12 others showed various levels of *ScFRK2* mRNA overexpression (*ScFRK2*-OX lines) (e.g. lines S2 and S17 in Fig. 3A). Plants containing the antisense construct showed reduced *ScFRK2* mRNA levels compared with the WT (data not shown), but none showed mRNA down-regulation as severe as the co-suppression line S20 (Fig. 3A). No obvious developmental defects were detected either in co-suppression line S20 or in the antisense lines. Overall plant growth and development appeared unaffected in all *ScFRK2*-OX transgenic lines. However, severe defects in seed and fruit development were exhibited. Half of the *ScFRK2*-OX lines (OX lines S2, S17, S5, S7, S9, and S11) produced smaller than normal fruits containing fewer seeds (Fig. 3B, C; Table I). Two OX lines, S2 and S17, were selected for detailed phenotypic observation because they exhibited the highest levels of *ScFRK2* mRNA. Development of the fruits started similarly in WT and transgenic lines, but significant differences in fruit size were detected from 10 DAP in OX lines (Fig. 3C). In WT *S. chacoense* plants, fruits develop to maturity in ~21 DAP. Thereafter, mature embryos start to desiccate in order to reach seed maturity at ~40 DAP. At 21 DAP, fruit diameters from *ScFRK2* transgenic lines reached only 60% of those of the normal WT fruits, weighed only 36% of the weight of normal WT fruits, and contained only 6.4% of the total number of seeds normally produced in WT fruits. The reduced seed set could explain the small fruit size observed. Furthermore, mature seeds obtained from OX lines bore embryos that were retarded in their development, most of them still being at the torpedo stage compared with mature embryos in WT plants (Table 1). These embryos would eventually proceed to a mature stage and plants could be regenerated from these when hand dissected and placed on a sterile solid MS medium (data not shown).

Table 1. *Comparison of fruit size, weight, ovule number, and embryo developmental stage between wild-type and mutant plants*

Plant	Fruit diameter (mm)[a]	Fruit fresh weight (g)[a]	No. of ovules per fruit[a]	21 DAP embryo mean developmental stage[b]
Wild-type G4	15.8±1.0	2.45±0.24	106.2±8.3	Mature
ScFRK2-S2	10.1±1.1	0.89±0.23	6.8±1.9	Torpedo

[a] Each number represents the mean value of 24 fruits ±SD.
[b] Developmental stage at which most embryos were found at 21 DAP, randomly taken from 24 dissected ovules. For the wild type, out of 24 embryos, 19 were mature and five were at the torpedo stage. For the *ScFRK2* S2, three embryos were at the heart stage, 13 at the torpedo stage, four at the walking-stick stage, and four at the mature embryo stage.

Further analyses of the *ScFRK2*-S2 and *ScFRK2*-S17 mutants revealed that overexpression of *ScFRK2* led to the transformation of ovules into carpelloid structures (CSs). In hand-dissected ovaries from the *ScFRK2*-OX lines, the uppermost ovules in the ovary developed as filiform structures (Fig. 4B). A normal size ovule in this transgenic background is also visible, indicated with a white arrow in Fig. 4B. By comparison, a WT ovary containing normal ovules is shown in Fig. 4A. Ovaries with a severe phenotype showed small bumps on their surface instead of a perfectly round and smooth surface as seen in control ovaries (data not shown). Inside these ovaries, the filiform

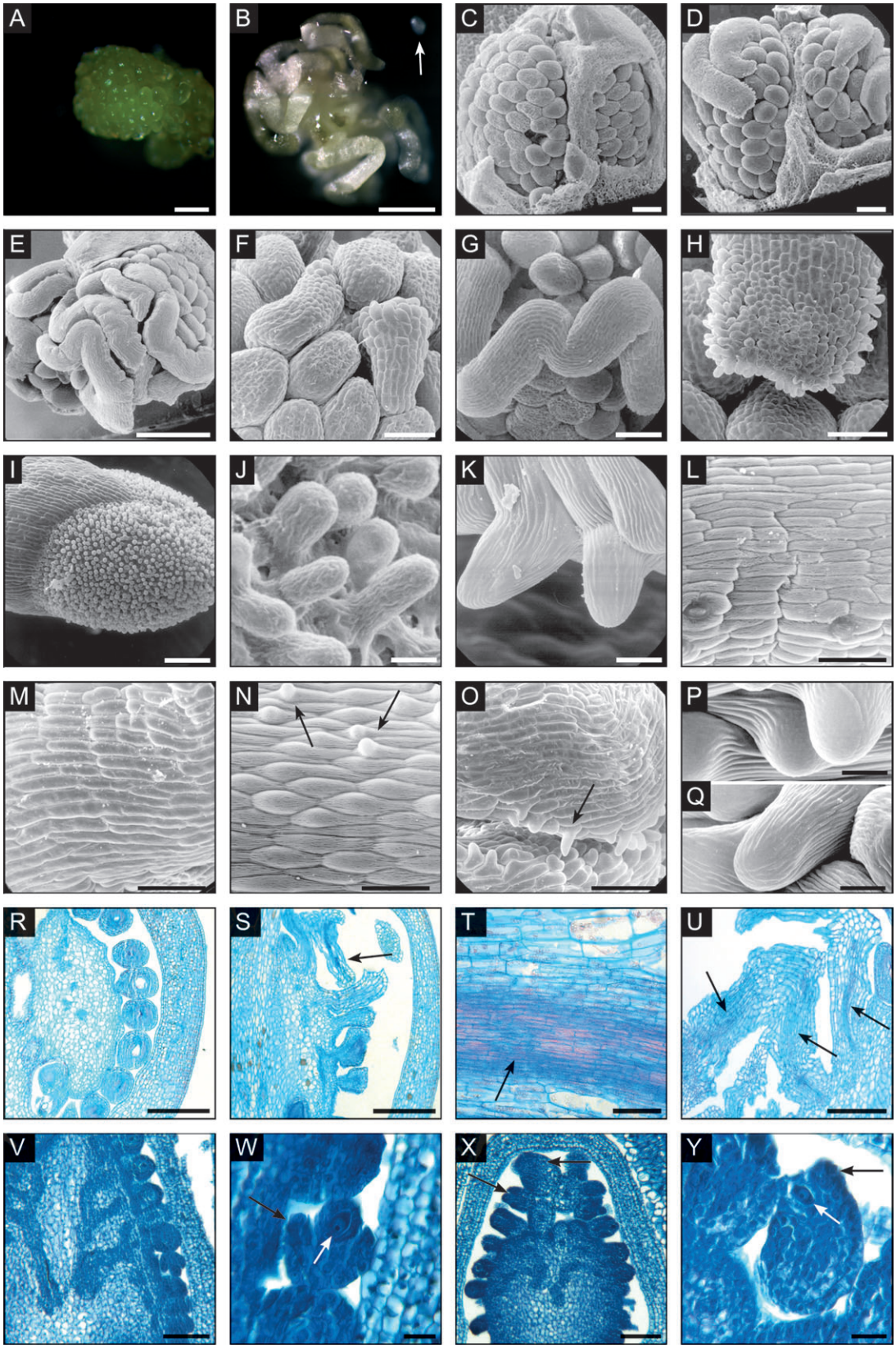

Fig. 4. Fruit and ovule development of *ScFRK2*-OX plants. (A and B) Wild-type (A) and transgenic (B) ovaries. The ovary wall has been removed to expose the ovules. The white arrow in B points to a normal ovule. (C–Q) SEM images from wild-type (C, I, J, L, N, and P) and transgenic (D–H, K, M, O, and Q) plants. (C) Ovules from a wild-type plant. (D and E) Ovules from *ScFRK2*-OX plants, with D showing a milder phenotype than E.

structures filled most of the locular space, leaving a few empty pockets. The transformed ovules took on a twisted spaghetti-like appearance due to the physical constraint of the available growth space in the ovary (Fig. 4B). To identify the nature of these transformed ovules, their morphology was analysed by SEM. WT ovaries showed well distributed ovules in the two locules (Fig. 4C). In contrast, mutant ovaries showed variable numbers of normal sized ovules and ovules with abnormal growth. The severity of the defect was also influenced by environmental factors, such as day length or temperature, with more abnormal ovules observed in warmer periods during summer in the greenhouse (data not shown). The length of these modified ovules varied from small outgrowths to long and thin structure (Fig. 4D–G). Figure 4D shows modified ovules with a mild phenotype, while Fig. 4E shows a more severe phenotype where filiform structures are longer and become twisted (Fig. 4G). These structures developed from the placenta as for normal ovules (Fig. 4F) and had an intrusive growth that disrupted ovule organization in their surroundings. Cells on the filiform structure were elongated without being wider than normal ovule cells (Fig. 4F). The tip of the filiform structure had cell projections (Fig. 4H) similar to stigmatic papillae found on WT pistils (Fig. 4I). As a comparison, a magnification of stigmatic papillae of a WT style is shown in Fig. 4J. The papillae on the filiform structure (Fig. 4K) resemble normal stigmatic papillae (Fig. 4J), except that no mucilage could be observed on their surface. Considering that the CS most probably corresponds to immature styles, this is not unexpected. Cell morphology was also compared between WT stylar and CS cells (Fig. 4L, N, and P, and M, O, and Q, respectively). Cells from CS (Fig. 4M) showed rectangular cells that were more similar to stylar cells (Fig. 4L) than to ovule cells. Moreover, CS shared the same smaller triangular cells found on stylar cells (data not shown), but lacked guard cells and stomata that mature styles show along their length (compare Fig. 4L and M). Another feature of *S. chacoense* style is the presence of small papillae-like protrusions that develops as the style matures (O'Brien *et al*., 2002*a*). Along their length, style (Fig. 4N) and CS (Fig. 4O) shared similar protruding papillae-like cells (Fig. 4N, O; black arrows). When magnified, these papillae-like cells showed similar cuticular ornamentations in both transgenic (Fig. 4Q) and WT cells (Fig. 4P).

To analyse the cell types present in the transformed ovules in more detail, thin sections of fixed ovaries from *ScFRK2*-OX plants were observed. The WT ovary contained ovules uniform in size and evenly arranged, extending from the placenta (Fig. 4R, only one locule shown). In contrast, ovaries in *ScFRK2*-OX plants contained irregularly shaped ovules as well as CSs similarly extending from the placenta (Fig. 4S, only one locule shown). The locule organization was disrupted due to an excessive growth of the long filiform CS (Fig. 4S). These CSs showed a clearly different cellular organization from WT ovules. Transverse sections through the CS revealed strands of thin, long, and more compacted cells (arrows in Fig. 4S, U), reminiscent of the transmitting tissue cells found in WT style (arrow in Fig. 4T). CSs contained vessels throughout almost the entire length of the filiform (Fig. 4S, U). This is also similar to the transmitting tract of the WT style. On the other hand, WT ovules contained vessels only in the funiculus (data not shown). An attempt was made to identify CS further using molecular markers for mature style-transmitting tissue (*S-RNase*, *HT* gametophytic self-incompatibility modifier) (O'Brien *et al*., 2002*b*). However, the signal intensities of the marker transcripts were about the same between WT and mutant ovaries (data not shown). This may be because these CSs are more similar to immature styles and the expression of these genes had not yet initiated. At this stage, CS did not contain any structures resembling an embryo sac. In the section shown in Fig. 4S, most ovules, including those that are normal sizes, appeared abnormal, and only a few would have led to seed formation, which explains the low seed yield in mature fruits (Table 1). At 7 DAP, the filiform CS had already started to wither and turn brown, and none could be observed at fruit maturity (data not shown).

The ontogeny of CS in developing pistils was investigated further. Ovule primordia of *ScFRK2*-OX plants appeared identical to those of WT plants (data not shown). The first ovule abnormalities were detected when integument growth became apparent. Instead of forming a single layer integument characteristic of *Solanum* species (Fig. 4W, black arrow), the stalk of ovule primordium

(F) Enlargement of emerging carpelloid structure (CSs). (G) Enlargement of an elongated CS. (H) Papillae on the CS extremity. (I) Papillae on a wild-type stigma. (J) Enlargement of WT stigmatic papillae. (K) Enlargement of papillae on the CS extremity. (L) Style cortex epidermis of a wild-type plant. (M) Epidermis of the stylar section of a CS. (N) Small papillae on a wild-type style 3 d before anthesis. (O) Small papillae from the stylar section of a CS. In N and O, papillar cells are indicated by dark arrows. (P) Enlargement of papillar ornamentations from the style of a wild-type plant. (Q) Enlargement of papillar ornamentations from a CS of a transgenic plant. (R–U) Light microscopy of wild-type (R, T) and transgenic (S, U) plants. (R) Ovary from a wild-type plant (only one locule shown). (S) Ovary from a *ScFRK2*-OX plant (only one locule shown). (T) Transverse section of a style from a wild-type plant. The arrow indicates the transmitting tract. (U) Transverse section of a CS showing dense cells resembling the transmitting tract (indicated by arrows). (V) Developing ovary from a wild-type plant. The section was taken from a flower bud ~2 mm in length. (W) Enlargement of one of the ovules shown in V. The black arrow indicates the ovule integument and the white arrow indicates the megasporocyte. (X) Developing ovary from a *ScFRK2*-OX plant. The section was taken from a flower bud ~2 mm in length. The black arrows indicate developing CSs. (Y) Enlargement of the tip of the CSs shown in X. The black arrow indicates the integument. Integuments were often enlarged. The white arrow indicates the megasporocyte. Scale bars, 1 mm (A and B); 100 μm (C, D, F–I, L–O, U, V, and X); 500 μm (E); 50 μm (T); 10 μm (J, K, P, and Q); 250 μm (R and S); 20 μm (W and Y).

continued to grow and expanded excessively, forming enlarged ovules (Fig. 4X, Y, black arrows). At this stage, the enlarged ovule still retained a structure resembling the nucellus containing a megasporocyte at the tip (Fig. 4Y, white arrow). Some megasporocytes were undergoing meiosis, which appeared relatively normal (data not shown), suggesting that the conversion to carpelloids initiates from abnormal growth of the integument and stalk. Since no structures that resembled the megasporocyte or megagametophyte were visible in mature CS (Fig. 4S, U), the megagametophyte may either have degenerated or have been engulfed by the outgrowth of its surrounding tissues.

Expression of the ScFRK2 *gene in developing ovules*

Since *ScFRK2* overexpression interfered with ovule development before fertilization (see above), the *ScFRK2* expression pattern was investigated further in developing ovules. RNA gel blot analyses using flower buds 1, 2, 3, 4, or 12 mm in length failed to detect any *ScFRK2* mRNA signals (data not shown), possibly because the cells expressing *ScFRK2* comprised only a small portion of the flower buds. However, RNA *in situ* hybridization revealed cell-specific accumulation of *ScFRK2* mRNA in early ovule development (Fig. 5). *ScFRK2* mRNA signals were detected in the ovule primordia of young pistils (Fig. 5B). Particularly intense signals were detected from the megasporocyte (Fig. 5D). Signals in the megasporocyte weakened as the ovule developed, and stronger signals were instead detected from the ovule integument (Fig. 5C). Intense signals were detected near the growing end of the ovule integument (Fig. 5C, E). Only diffuse signals were detected in the ovule integument after the integument reached full growth, and little or no signal was detected from megagametophytes (Fig. 2CII).

As expected, *ScFRK2* mRNA signals were stronger in *ScFRK2*-OX plants than in WT plants (compare Fig. 5G and H). Surprisingly, transgenic plants retained a spatial expression pattern of *ScFRK2* that somewhat resembled the WT, i.e. strong expression in gametophytes. Ovule-specific signals in the transgenic plant are shown in Fig. 5H. However, there were distinct differences in the cell specificity of *ScFRK2* distribution. Developing ovules of transgenic plants retained high levels of *ScFRK2* mRNA in megasporocytes (Fig. 5H, I), whereas little or no signal was detected in the megasporocytes of WT ovules (Fig. 5C, E, G). Much weaker signals were detected in the stalk of developing CS, while intense signals were always associated with the megasporocyte and its surrounding tissues at the tip (Fig. 5H).

The expression of ScFBP11*, a* Solanum *orthologue of* FBP7 *and* FBP11*, is altered in* ScFRK2*-OX plants*

In *Petunia*, down-regulation of the class D MADS-box genes *FBP7* and *FBP11* changes the fate of the ovule primordium to a carpel primordium and spaghetti-like structures in positions normally occupied by ovules (Angenent *et al*., 1995). These abnormal structures morphologically resemble style and stigma tissues, like the ones obtained in *ScFRK2*-OX lines. To determine if *ScFRK2* overexpression affected the expression of the class D MADS-box gene, an EST corresponding to a putative *FBP7/11* orthologue from the *S. chacoense* ovary library was isolated and termed *ScFBP11*. ScFBP11 shares 87% amino acid sequence identity with both FBP7 and 11, and 86% with TAGL11, a tomato FBP7/11 orthologue (Busi *et al*., 2003). A phylogenetic analysis confirmed the close association of *ScFBP11* with *Petunia* FBP7 and FBP11 as well as with other class D MADS-box genes (data not shown). *In situ* RNA hybridization was performed using a partial *ScFBP11* cDNA sequence to determine the spatial expression pattern of *ScFBP11*. In WT plants, diffuse *ScFBP11* mRNA signals were detected in the integument of the developing ovule, and weak or no signals were detected from megasporocytes (Fig. 5K). *ScFBP11* appeared to be up-regulated in the developing ovule of *ScFRK2*-OX transgenic plants. Ovule signals were much stronger in transgenic plants than in WT plants (compare Fig. 5L and K). More importantly, transgenic ovules retained *ScFBP11* signals in megasporocytes (Fig. 5N), in striking contrast to WT ovules (compare Fig. 5M and N). Developing CSs retained intense signals in megasporocytes at the tip, while signals were mostly absent from the stalk (Fig. 5L).

cDNA microarray analyses

To determine whether the overexpression of *ScFRK2* showed any alterations in the expression of other genes, the mutant plants were compared with WT *S. chacoense* plants using DNA microarrays from a 7.7 K array made from ovule-derived ESTs (Germain *et al*., 2005). ANOVA (analysis of variance) testing was used, along with a Benjamini and Hochberg multiple testing correction algorithm, to select 389 ESTs that showed a statistically significant difference in transcript abundance between the WT and the *ScFRK2*-overexpressing ovules. A Welch *t*-test ($P < 0.05$) was initially used to compare the profiles from the *ScFRK2* versus control and the control versus control comparisons. They were then further restricted with a 1.5-fold variation (1.5 cut-off up or down). A relatively even split was observed between up-regulated (160) and down-regulated (213) transcripts, and this result is presented in Supplementary Table S1 at *JXB* online. The observed changes in transcript abundance are relatively modest compared with what has been observed in other experiments (time-course analysis following fertilization in WT plants; data not shown). Since the phenotype in *ScFRK2*-OX lines is only observable in a fraction of the samples (see Fig. 4, showing ovules at different stages of transformation into CS structures in the same ovary), it is possible that the

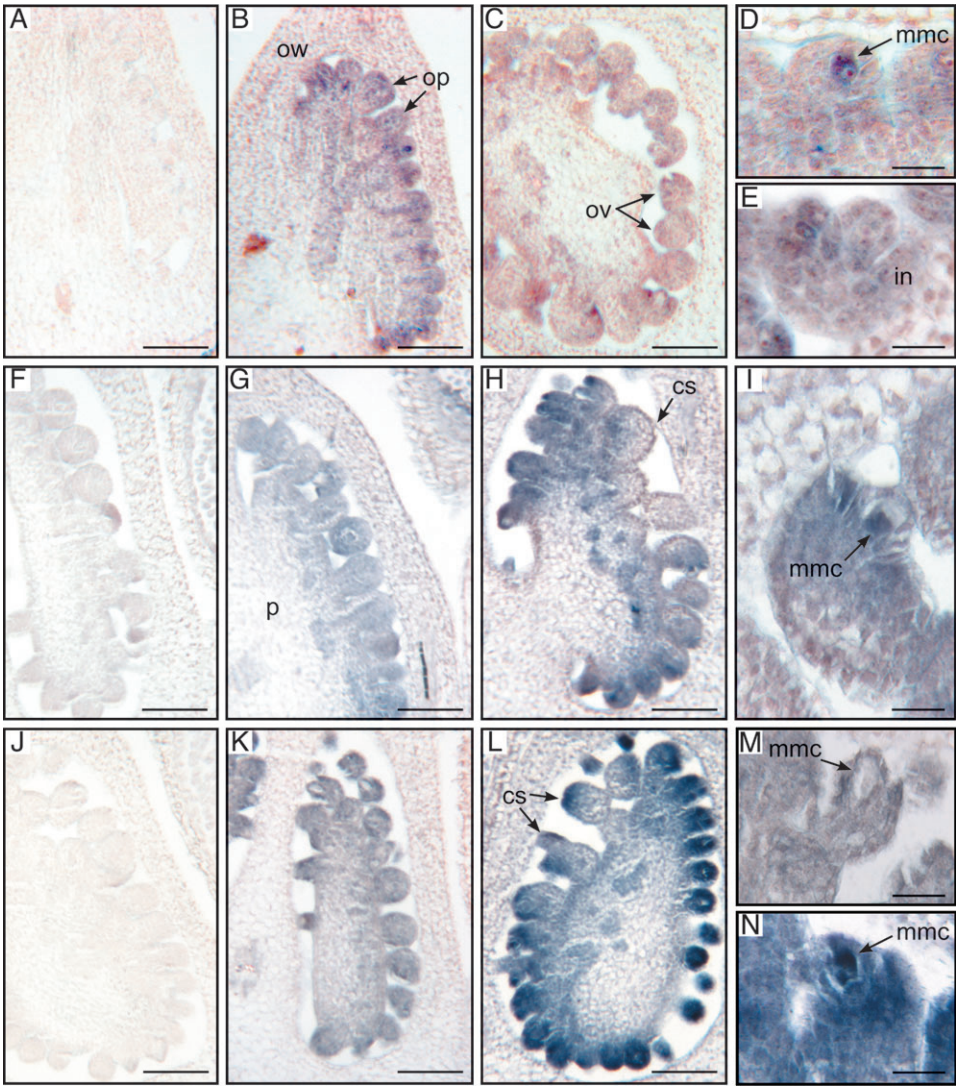

Fig. 5. *In situ* RNA hybridization analyses in developing ovules. (A–E) *ScFRK2* expression in wild-type plants. (A) Sense probe. (B–E) Antisense probe. (A and B) A developing ovary showing ovule primordia arising from the placenta. Sections were taken from a flower bud ~1.5 mm in length. (C) Ovary at a later stage showing a developing ovule with growing integuments. The section was taken from a flower bud ~2 mm in length. As ovules mature, the signal in the megasporocyte became weaker while the signal in the integument became stronger, particularly at the growing tip. (D) Enlargement of B showing an intense *ScFRK2* mRNA signal in the megasporocyte. (E) Enlargement of C. (F–I) Comparison of *ScFRK2* expression between wild-type and *ScFRK2*-OX plants. *In situ* RNA hybridization was performed simultaneously using identical conditions to allow direct comparison. Sections were taken from ovaries at a similar stage to those shown in C. (F) Sense probe. (G–I) Antisense probe. (F and G) Wild-type plant. (H) *ScFRK2*-OX plant. Arrows show developing CSs. Although signals are almost absent from the stalk, intense signals remain strong at the tip. (I) Enlargement of H, showing the megasporocyte at the tip of the developing CS. The signal in the megasporocyte remains strong. (J–N) *ScFBP11* expression in developing ovules. Tissue sections were taken from ovaries at about the same stage as those in C–I. *In situ* RNA hybridization was performed simultaneously using identical conditions to allow direct comparison. (J) Sense probe. (K–N) Antisense probe. (J and K) Wild-type plant. (K) Diffuse signals were detected from the ovule integument while weak signals were detected from the megasporocyte. (L) Ovary from a *ScFRK2*-OX plant. Strong signals were detected in ovules that appear normal and also at the tip of the developing CS. Very weak signals were detected in the stalk of the CS. (M) Enlargement of K, showing the absence of signal in the megasporocyte. (N) Enlargement of L, showing intense signals in the megasporocyte of the CS. cs, carpelloid; in, integument; mmc, megasporocyte; op, ovule primodium; ov, ovule; ow, ovary wall; p, placenta. Scale bars, 100 μm (A–C, F–H, J–L); 20 μm (D, E, I, M, and N).

changes in transcript abundance are somewhat 'diluted' by contributions from unaffected tissue. Furthermore, for the microarray experiment, whole ovaries were used instead of isolated ovules, increasing the dilution effect. Nevertheless, statistically significant results were obtained for 373 ESTs. To determine whether the differentially expressed genes were involved in similar biological processes, these were categorized according to their gene ontology (GO) classification. Apart from a large class of hypothetical/unknown proteins (23.7%), the largest functional groups observed were implicated in metabolism (17.5%), proteins with binding function, including RNA, DNA, protein, and ion binding (9.8%), development and organogenesis (8.5%), protein synthesis (7%), defence response-related

proteins (6.9%), protein fate (8.5%), signal transduction (3.3%), transcription (5.1%), and transport (4.3%). Interestingly, of the selected genes, some have previously been shown to be involved in flower or fruit development. In the *ScFRK2*-OX downregulated category, among the genes involved in transcriptional regulation, homologues of LEUNIG and EIL2 transcription factors have been found. LEUNIG has been shown to regulate AGAMOUS negatively during flower development (Conner and Liu, 2000), while EIL2 (ETHYLENE INSENSITIVE3-like) is involved in ethylene perception, flower abscission, and fruit ripening (Tieman *et al*., 2001). Among the genes involved in signal transduction in the down-regulated category, three RLKs from *S. chacoense*, ORK3, 12, and 23, and an ethylene receptor homologue have been found. ORK3 and 12 transcript levels had been shown to increase after fertilization in the ovary, while transcript levels for ORK23 were induced at a distance in the ovary by pollination alone (Germain *et al*., 2005). In the *ScFRK2*-OX up-regulated category, two RLKs and one serine/threonine kinase with possible involvement in developmental processes were retrieved. The ORK6 RLK from *S. chacoense* was previously shown to be strongly induced (17-fold) following fertilization in ovaries (Germain *et al*., 2005), while the second EST had significant sequence identity with putative orthologues of the phytosulphokine (PSK) receptor. PSKs are small peptide ligands that induce plant cells to dedifferentiate and re-enter the cell cycle at nanomolar concentrations (Matsubayashi *et al*., 2002). Two PSK genes in maize, ZmPSK1 and ZmPSK3, were also detected in egg and central cells of the female gametophyte, while ZmPSK1 mRNA was present in synergids, indicating that the PSK peptide probably plays a role during gametogenesis and fertilization (Lorbiecke *et al*., 2005). The other protein kinase was most similar to the APK1a kinase, a kinase very similar to the APK2a kinase, whose gene was originally isolated as having *cis*-regulatory elements bound by AGAMOUS through an *in vivo* binding assay (Ito *et al*., 1997).

Discussion

ScFRK2 belong to the MEKK family of MAPKKKs

Using the basic local alignment search tool on publicly available databases, both ScFRK1 and ScFRK2 were found to be most similar to the catalytic domain of numerous MAPKKKs, as well as to three uncharacterized protein kinases from *A. thaliana* (MAPKKK19, 20, and 21). When compared with most MAPKKK family members, these protein kinases (ScFRK1 and -2, and MAPKKK19, 20, and 21) lacked a typical regulatory domain. A phylogenetic analysis confirmed that these five MAPKKKs belonged to the same subgroup inside the MEKK family of MAPKKKs. Although kinase activity could be obtained from the ScFRK1 and ScFRK2 kinases after *in vitro* translation (data not shown), complementation in a yeast mutant background deficient for the Ste11 MAPKKK could not be achieved with either kinase (data not shown). This suggests that they may not be involved in a typical MAPK cascade, and/or that the lack of a large N-terminal regulatory domain, like in Ste11, might hamper proper function in yeast and make complementation ineffective.

Developmental defects caused by overexpression of ScFRK2

Overexpression of the *ScFRK2* gene leads to developmental defects in ovules, and delayed seed and fruit development. Although ectopic expression can sometime lead to pleiotropic effects on plant development, phenotypic abnormalities were found only in developing ovule and pollen (O'Brien *et al*., 2007) where *ScFRK2* was most strongly expressed during normal development. Ectopic expression of *ScFRK2* in vegetative tissues did not cause any visible changes in vegetative development. This suggests that the ScFRK2 kinase acts only on the cells that contain its cognate signalling pathway partners and targets. Specific effects of *ScFRK2* overexpression may be explained partly by the ovule-specific accumulation of *ScFRK2* mRNAs in transgenic plants (Fig. 5H). Although one would expect the activity of the CaMV 35S promoter to be more ubiquitous, some tissue preferences have been reported previously (Wilkinson *et al*., 1997). Alternatively, the coding region of the *ScFRK2* gene might itself contain regulatory elements curbing the expression pattern obtained in ovules under the CaMV 35S promoter. In addition, steady-state *ScFRK2* mRNA levels may be controlled post-transcriptionally by affecting mRNA processing and stability. Also, there may be a positive feedback mechanism that promotes up-regulation of endogenous *ScFRK2* transcription.

Nevertheless, there were distinctive differences in the *ScFRK2* mRNA accumulation pattern in developing ovules between WT and transgenic plants. A schematic representation of *ScFRK2* mRNA distribution is shown in Fig. 6. In WT plants, *ScFRK2* mRNA signals in megasporocytes weakened after integument initiation while maintaining mRNA levels in integuments (Fig. 5C, E, and G). In contrast, megasporocytes of transgenic ovules, including those that appeared of normal size, maintained high levels of *ScFRK2* mRNAs (Fig. 5H, I). The abnormal elevation of *ScFRK2* in megasporocytes may hinder ovule maturation processes, possibly by preventing megagametogenesis and integument differentiation. This may be the reason why most ovules, including normal sized ones, failed to mature in *ScFRK2*-OX plants (Fig. 4S). There were few *ScFRK2* mRNA signals in the stalk of developing CSs (Fig. 5H, I). It is unlikely that the absence of *ScFRK2* is the cause of loss of ovule identity because *ScFRK2* down-regulation either

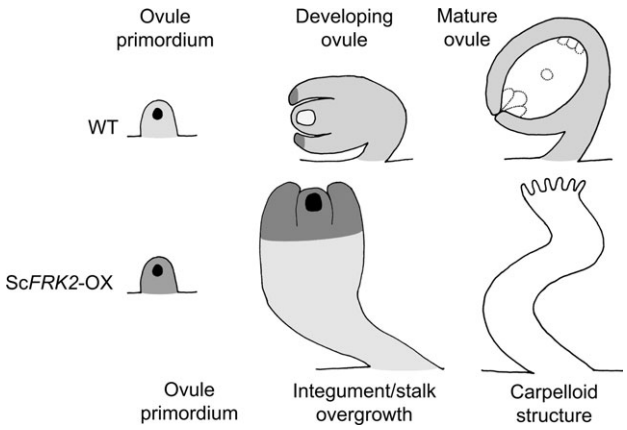

Fig. 6. Schematic representation of *ScFRK2* mRNA distribution during wild-type and *ScFRK2-OX* ovule development. *ScFRK2 in situ* RNA hybridization signal distribution is represented by the grey scale, where black is strongest, and decreasing grey intensity corresponds to lower expression levels. Wild-type. *ScFRK2* mRNA accumulates in the megasporocyte during ovule primordium formation. As ovules mature, *ScFRK2* mRNA levels decrease in megasporocyte and increase near the growing tip of the ovule's integument. When ovules reach maturity, *ScFRK2* mRNA is only detected in the integument. *ScFRK2*-OX. In general, *ScFRK2* mRNA accumulates more than the wild type but the accumulation pattern during ovule primordium formation is identical to that of the wild type (i.e. accumulation mostly found in megasporocyte). *ScFRK2* mRNA remains abundant in megasporocyte during ovule/CS formation. Also, *ScFRK2* mRNA accumulates at the tip of overgrowing integument, whereas no or little *ScFRK2* mRNA is detected in the overgrowing funiculus (stalk of the CS).

by antisense or by co-suppression does not cause ovule abnormality (see above). Instead, the down-regulation may have been caused by the loss of ovule identity itself. The abnormal elevation of *ScFRK2* in megasporocytes may have triggered the loss of identity in the integument, which in turn down-regulates *ScFRK2* expression in the CS. This scenario is also consistent with the persistence of *ScFRK2* mRNA in the nucellus-like structures at the tip of the CS. Once the programme for CS formation is initiated, the CS may have taken over the entire ovule to eliminate any structures reminiscent of megasporocytes or megagametophytes.

The *ScFRK2* expression in pistils prior to fertilization, taken together with a strong increase in expression observed in ovaries immediately after fertilization, suggests that this protein kinase has both pre- and post-fertilization roles. Unfortunately, the role of ScFRK2 in post-fertilization ovule development could not be assessed thoroughly in this study since overexpression leads to the homeotic conversion of ovules into CSs that did not give rise to seeds. The few seeds that were obtained exhibited delayed development (Table 1). Although this is consistent with the ScFRK2 function in post-fertilization ovule development, it is difficult to distinguish a direct effect on embryo development from an indirect effect due to pre-fertilization ovule deficiency. To study the role of ScFRK2 in post-fertilization ovule development, it will be necessary to direct *ScFRK2* expression only after fertilization using either a tissue-specific promoter or an inducible promoter.

Down-regulation of *ScFRK2* via antisense inhibition or co-suppression should have been more informative; however, no obvious defects were observed in these transgenic plants (data not shown). One explanation for this is functional redundancy shared with other related genes. The presence of such gene(s) was suggested by the DNA gel blot analysis (Fig. 2A). It will be interesting to see the effects of dominant-negative mutations, which may overcome the functional redundancy problem. In this regard, it should be noted that the effect of *ScFRK2* overexpression may not always result in the enhancement of the normal ScFRK2 function. Proteins involved in MAPK cascades often function in protein complexes where MAPKKKs, MAPKKs, and MAPKs are anchored together and phosphorylate its targets within the complex (Murphy and Blenis, 2006). Overexpression of one component may not always enhance the function of its complex as a whole. In an extreme situation, the presence of excess proteins that do not participate in its cognate complex may actually hinder the complex function by competing for the same upstream targets. It is not known whether *ScFRK2* overexpression enhances or inhibits its downstream functions. Neither is it known whether *ScFRK2* overexpression results in accumulation of active ScFRK2 kinase. It will be necessary to identify downstream target proteins of ScFRK2. ScFRK2 function can then be monitored through the phosphorylation status of the target proteins.

Cells in multicellular organisms are equipped with an intricate network of signalling pathways that may interact to maintain a delicate balance of cell fate determination. This is why, unlike mutations in transcription factors, mutations in signalling pathways are difficult to interpret. Interplay of different MAPK cascades is illustrated by interactions between SIPK and WIPK, two closely related MAPKs in tobacco. Both SIPK and WIPK are phosphorylated after exposure to ozone, which triggers production of reactive oxygen species scavengers (Samuel and Ellis, 2002). Stable overexpression of SIPK does not result in accumulation of phosphor-SIPK. SIPK is phosphorylated only after the exposure to ozone and, even then, the amount of phosphor-SIPK is no more than in the WT. An unexpected side-effect of SIPK overexpression was instead found in the phosphorylation status of WIPK. SIPK overexpression inhibits accumulation of phosphor-WIPK and, as a result, cells become hypersensitive to ozone stress. Inhibition of SIPK via RNA interference (RNAi) also results in hypersensitivity to ozone. In this case, phosphor-WIPK accumulation is stimulated while phosphor-SIPK accumulation is inhibited (Samuel and Ellis, 2002). Does the FRK2 pathway interact with other pathway(s) in a similar manner? Future biochemical analyses should reveal the web of FRK2 signalling pathways on ovule fate determination.

Gene mutations that result in loss of ovule identity

Overexpression of *ScFRK2* resulted in homeotic conversion of ovules into CSs (Fig. 4). Several genes coding for transcription factors have been identified as regulators of ovule development (Schneitz *et al*., 1997; Gasser *et al*., 1998), and misexpression of some of these genes leads to reiteration of carpel development instead of ovules to form CSs and thus cause the loss of ovule identity. In many cases, the loss of ovule identity can be linked to either the misexpression of a class C MADS-box gene or down-regulation of class C and/or D MADS-box genes. In *Arabidopsis*, a mutation in *APETALA2* (*AP2*), a negative regulator of the class C MADS-box gene *AGAMOUS* (*AG*), causes the conversion of ovule to CSs within the gynoecium although at a low frequency (Modrusan *et al*., 1994). *BELL1* (*BEL1*) is also postulated as a negative regulator of *AG* (Ray *et al*., 1994). The *bel1* mutation likewise causes the loss of ovule identity, albeit with different timing to the *ap2* mutant (Modrusan *et al*., 1994). In the *bel1* mutant, the ovule integument continues to grow and differentiate into structures with carpel-like morphology (Modrusan *et al*., 1994). In the *ap2* mutant, homeotic conversion occurs at an earlier stage than in *bel1* mutants, as the CS forms directly from an ovule primordium projection (Modrusan *et al*., 1994). *AG* is misexpressed in both *ap2* and *bel1* mutants, and this may have caused the loss of ovule identity (Drews *et al*., 1991; Ray *et al*., 1994). Consistent with this idea, ectopic expression of *AG* orthologues results in homeotic conversion of ovule to CS in *Arabidopsis* (Ray *et al*., 1994) and tobacco (Mandel *et al*., 1992). Interestingly, the frequency of transformation in the *bel1* mutant decreases with decreasing temperatures, as well as with reducing day length (Modrusan *et al*., 1994). Ovule to CS conversion in the *ScFRK2*-OX lines was also influenced by temperature and day length (data not shown).

Involvement of the class D MADS-box genes in ovule identity determination was first identified in *Petunia*, a Solanaceae species like *S. chacoense*. Down-regulation of the class D MADS-box genes *FBP7* and *FBP11* via co-suppression changes the fate of the ovule primordia to the carpel primordia. Hence, CSs develop on the placenta (Angenent *et al*., 1995). *FBP7* and *FBP11* work redundantly because neither an *FBP7* nor an *FBP11* single knockout mutant causes a similar phenotype (Vandenbussche *et al*., 2003). Normally, the expression of *FBP7* and *11* mRNAs is found in carpels. However, ectopic expression of the *FBP11* gene causes ectopic ovule formation in the sepal, suggesting that *FBP11* is sufficient for ovule induction (Colombo *et al*., 1995). The *Arabidopsis* genome contains only one gene, *SEEDSTICK* (*STK*), that belongs to the class D MADS-box gene clade (Kramer *et al*., 2004). *STK* alone does not determine ovule identity but, instead, acts redundantly with three closely related class C MADS-box genes, *AG*, *SHATTERPROOF1* (*SHP1*) and 2 (*SHP2*) (Pinyopich *et al*., 2003). In the *shp1 shp2 stk* triple mutant, ovules are converted into carpel- or leaf-like structures with style-like characteristics (Pinyopich *et al*., 2003). Similar to *FBP11* in *Petunia*, ectopic expression of *STK*, *SHP1*, or *SHP2* in *Arabidopsis* causes conversion of sepals to carpelloid organs with ectopic ovules (Favaro *et al*., 2003). Interplay of class C and D MADS-box genes has further been demonstrated by protein interaction assays. Yeast two-hybrid and three-hybrid analyses have shown that when the class E MADS-box transcription factor SEPALLATA 3 (SEP3) is present, AG forms a complex with either STK, SHP1, or SHP2, and this complex (AG–SEP3–STK, AG–SEP3–SHP1, or AG–SEP3–SHP2) may be sufficient for promoting ovule identity (Favaro *et al*., 2003). Similarly, FBP11 forms a higher order complex with FBP2 (class E) and FBP6 (class C) transcription factors (Tonaco *et al*., 2006).

Possible interactions between ScFRK2 and FBP7/11 and/or AG pathways

The *ScFRK2* expression pattern in *S. chacoense* ovules was very similar to those of *FBP7* and *FBP11* in *Petunia* and *ScFBP11* in *S. chacoense*. Before fertilization, *ScFRK2* mRNAs are detected in ovule primordia in the young ovary (Fig. 5B) and ovule integuments of the mature ovary (Fig. 5C). Similarly, in *Petunia*, *FBP11* mRNA is detected in ovule primordia of the young ovary and the integuments of mature ovules (Angenent *et al*., 1995). A similar distribution of *ScFBP11* mRNA was observed in *S. chacoense* ovules (Fig. 5K). *ScFRK2* mRNA levels in ovules increased greatly after fertilization (2 DAP) and decreased back to pre-fertilization levels by 4 DAP (Fig. 2B, C). *Petunia FBP7* and *FBP11* mRNA levels in ovules also increase after fertilization (Colombo *et al*., 1997). However, unlike *ScFRK2*, the levels of *FBP7* and *FBP11* remain high for several days and decrease after 7 DAP (Colombo *et al*., 1997).

ScFRK2-overexpressing plants exhibit strikingly similar ovule defects to *FBP7*/*11* co-suppressed plants. In the ovary, ovules were transformed into filiform CSs, with the uppermost ovules being more frequently transformed. An identical situation was also found in the *Petunia FBP7*/*11* co-suppression lines (Angenent *et al*., 1995). The filiform structures exhibit characteristics similar to the style, such as structures resembling transmitting tracts and cell projections at the extremity resembling stigmatic papillae (Fig. 4K). These were also characteristics found in CSs of *FBP7*/*11* co-suppressed plants (Angenent *et al*., 1995). The only difference is that the CSs found in *FBP7*/*11* co-suppressed plants were devoid of any structures resembling the nucellus (Angenent *et al*., 1995), whereas nucellus-like structures were found in the *ScFRK2*-overepressing ovules at the beginning of abnormal growth (Fig. 4Y). This suggests that ScFRK2 may be acting on ovule development at a later stage than FBP7/11.

FBP11 accumulation following fertilization has been associated with its role in seed development. Endosperm development is altered in *FBP7/11* co-suppression lines (Colombo *et al*., 1997). Between the time of pollination, and up to 9 DAP, seed development is unaffected. However, later on, the endothelium of the ovule starts to degenerate. By 18 DAP, the endothelium completely degenerates, which leads to a disturbance of endosperm development and delayed embryo development (Colombo *et al*., 1997). *ScFRK2*-overexpressing lines also exhibited a delay in embryo development. WT fruits 21 DAP contained a large proportion of mature embryos, the remaining embryos being at the walking-stick stage. In *ScFRK2*-OX lines, embryo development was delayed, and at 21 DAP, most embryos are still at the late torpedo stage (Table 1). Although only a few ovules develop to mature seeds (around six per fruit compared with >100 seeds in WT plants), this delay has been consistently and repeatedly observed. These embryos would normally correspond to the ones observed 16–17 DAP in a WT plant. A small fruit phenotype was also observed (Fig. 3B, C). Mutations in *STK*, an *Arabidopsis* orthologue of *FBP7/11*, also cause defects in fruit (silique) development (Pinyopich *et al*., 2003).

Phenotype similarities between *ScFRK2*-OX plants and *FBP7/11* co-suppressed plants suggested that *ScFRK2* may be interfering with the function of class D MADS-box genes. Contrary to expectations, *ScFRK2* overexpression resulted in up-regulation of *ScFBP11* (Fig. 5L). If *ScFBP11* is up-regulated in *ScFRK2-OX* plants, how do they phenocopy *FBP7/11* down-regulated plants and *AG* up-regulated plants? There are at least two possible explanations for this apparent discrepancy. First, upregulation of *ScFBP11* may cause ectopic expression of an *AG* orthologue, which subsequently may cause ovule to CS conversion in transgenic plants. In *Arabidopsis*, ectopic expression of the class D gene *STK* causes ectopic accumulation of *AG* transcripts (Favaro *et al*., 2003). Unfortunately, no information is available regarding the expression levels of *AG* orthologues, because *AG* orthologues have not been cloned from *S. chacoense*. Secondly, ectopically expressed *ScFBP11* may take on *AG* function due to functional redundancy between class C and D MADS-box genes. Functional redundancy between class C and D genes has been reported in *Arabidopsis* in which loss of ovule identity occurs only when both C and D gene functions are lost (Pinyopich *et al*., 2003). Furthermore, *35S::STK* partially restores *AG* function in *ag1* mutants (Favaro *et al*., 2003). In either case, the fact that *ScFBP11* expression was altered by *ScFRK2* overexpression suggests that there are at least some interactions, direct or indirect, between the *ScFRK2* and *ScFBP11* pathways.

To identify further target genes of the *ScFRK2* pathway, global changes in gene expression levels were examined in transgenic plants using a microarray analysis. Genes differentially regulated between transgenic and wild-type ovaries were identified (see supplementary Table 1 at *JXB* online). Particularly interesting is the down-regulation of *LEUNIG* (*LUG*) in *ScFRK2*-OX ovaries. The *lug* mutation was initially identified as an enhancer of *ap2* mutant defects (Liu and Meyerowitz, 1995). Like *ap2* and *bel1* mutation, *lug* mutation causes ectopic expression of *AG*, suggesting that *LUG* is a negative regulator of *AG* (Liu and Meyerowitz, 1995). The *lug* mutation alone causes abnormal gynoecium development where two carpel valves remain open (Liu *et al*., 2000). *LUG* mRNA accumulation in ovules suggests that *LUG* is also involved in ovule development (Conner and Liu, 2000). *LUG* works redundantly with *AINTEGUMENTA* (*ANT*), another negative regulator of *AG*, to control ovule development. Double mutants of *lug* and *ant* cause complete abolishment of ovules as well as other marginal tissues of the gynoecium (Liu *et al*., 2000). Down-regulation of a *LUG* orthologue predicts up-regulation of an *AG* orthologue in the transgenic plants and is consistent with the ovule phenotype. However, further identification and expression analyses of *AG* orthologues will be necessary to confirm this point. Finally, it will be interesting to know if any of the differentially expressed genes are regulated by class C or D MADS-box genes.

Supplementary data

Supplementary data are available at *JXB* online.

Acknowledgements

We thank Dr Malcolm Whiteway (Biotechnology Research Institute, NRC, Montréal, Canada) for providing the *ste*11 mutant yeast strain and Gabriel Téodorescu for plant care and maintenance. We also thank Simon Joly for his help and advice regarding the phylogenetic analysis. This work was supported by the Natural Sciences and Engineering Research Council of Canada (NSERC, Canada) and by le Fonds Québécois de la Recherche sur la Nature et les Technologies (FQRNT, Québec). MO is the recipient of PhD fellowships from NSERC and from FQRNT. DPM holds a Canada Research Chair in Functional Genomics and Plant Signal Transduction.

References

Angenent GC, Franken J, Busscher M, van Dijken A, van Went JL, Dons HJ, van Tunen AJ. 1995. A novel class of MADS box genes is involved in ovule development in petunia. *The Plant Cell* **7,** 1569–1582.

Asai T, Tena G, Plotnikova J, Willmann MR, Chiu WL, Gomez-Gomez L, Boller T, Ausubel FM, Sheen J. 2002. MAP kinase signalling cascade in Arabidopsis innate immunity. *Nature* **415,** 977–983.

Becraft PW. 2002. Receptor kinase signaling in plant development. *Annual Review of Cell and Developmental Biology* **18,** 163–192.

Becraft PW, Asuncion-Crabb Y. 2000. Positional cues specify and maintain aleurone cell fate in maize endosperm development. *Development* **127,** 4039–4048.

Bergmann DC, Lukowitz W, Somerville CR. 2004. Stomatal development and pattern controlled by a MAPKK kinase. *Science* **304,** 1494–1497.

Busi MV, Bustamante C, D'Angelo C, Hidalgo-Cuevas M, Boggio SB, Valle EM, Zabaleta E. 2003. MADS-box genes expressed during tomato seed and fruit development. *Plant Molecular Biology* **52,** 801–815.

Bussière F, Ledû S, Girard M, Héroux M, Perreault J-P, Matton DP. 2003. Development of an efficient *cis–trans–cis* ribozyme cassette to inactivate plant genes. *Plant Biotechnology Journal* **1,** 423–435.

Canales C, Bhatt AM, Scott R, Dickinson H. 2002. EXS, a putative LRR receptor kinase, regulates male germline cell number and tapetal identity and promotes seed development in Arabidopsis. *Current Biology* **12,** 1718–1727.

Chevalier D, Batoux M, Fulton L, Pfister K, Yadav RK, Schellenberg M, Schneitz K. 2005. STRUBBELIG defines a receptor kinase-mediated signaling pathway regulating organ development in Arabidopsis. *Proceedings of the National Academy of Sciences, USA* **102,** 9074–9079.

Clark SE, Running MP, Meyerowitz EM. 1993. CLAVATA1, a regulator of meristem and flower development in Arabidopsis. *Development* **119,** 397–418.

Colombo L, Franken J, Koetje E, van Went J, Dons HJ, Angenent GC, van Tunen AJ. 1995. The petunia MADS box gene FBP11 determines ovule identity. *The Plant Cell* **7,** 1859–1868.

Colombo L, Franken J, Van der Krol AR, Wittich PE, Dons HJ, Angenent GC. 1997. Downregulation of ovule-specific MADS box genes from petunia results in maternally controlled defects in seed development. *The Plant Cell* **9,** 703–715.

Conner J, Liu Z. 2000. LEUNIG, a putative transcriptional corepressor that regulates AGAMOUS expression during flower development. *Proceedings of the National Academy of Sciences, USA* **97,** 12902–12907.

Drews GN, Bowman JL, Meyerowitz EM. 1991. Negative regulation of the Arabidopsis homeotic gene AGAMOUS by the APETALA2 product. *Cell* **65,** 991–1002.

Elion EA. 2000. Pheromone response, mating and cell biology. *Current Opinion in Microbiology* **3,** 573–581.

Fanger GR, Gerwins P, Widmann C, Jarpe MB, Johnson GL. 1997. MEKKs, GCKs, MLKs, PAKs, TAKs, and tpls: upstream regulators of the c-Jun amino-terminal kinases? *Current Opinion in Genetics and Development* **7,** 67–74.

Favaro R, Pinyopich A, Battaglia R, Kooiker M, Borghi L, Ditta G, Yanofsky MF, Kater MM, Colombo L. 2003. MADS-box protein complexes control carpel and ovule development in Arabidopsis. *The Plant Cell* **15,** 2603–2611.

Gasser CS, Broadhvest J, Hauser BA. 1998. Genetic analysis of ovule development. *Annual Review in Plant Physiology and Plant Molecular Biology* **49,** 1–24.

Germain H, Rudd S, Zotti C, Caron S, O'Brien M, Chantha S-C, Lagacé M, Major F, Matton DP. 2005. A 6374 unigene set corresponding to low abundance transcripts expressed following fertilization in *Solanum chacoense* Bitt., and characterization of 30 receptor-like kinases. *Plant Molecular Biology* **59,** 513–529.

Gifford ML, Dean S, Ingram GC. 2003. The Arabidopsis *ACR4* gene plays a role in cell layer organisation during ovule integument and sepal margin development. *Development* **130,** 4249–4258.

Hanks SK, Hunter T. 1995. Protein kinases 6. The eukaryotic protein kinase superfamily: kinase (catalytic) domain structure and classification. *FASEB Journal* **9,** 576–596.

Hanks SK, Quinn AM. 1991. Protein kinase catalytic domain sequence database: identification of conserved features of primary structure and classification of family members. *Methods in Enzymology* **200,** 38–62.

Hecht V, Vielle-Calzada JP, Hartog MV, Schmidt ED, Boutilier K, Grossniklaus U, de Vries SC. 2001. The Arabidopsis SOMATIC EMBRYOGENESIS RECEPTOR KINASE 1 gene is expressed in developing ovules and embryos and enhances embryogenic competence in culture. *Plant Physiology* **127,** 803–816.

Hirt H. 2000. MAP kinases in plant signal transduction. *Results of Problems in Cell Differentiation* **27,** 1–9.

Huson DH, Bryant D. 2006. Application of phylogenetic networks in evolutionary studies. *Molecular Biology and Evolution* **23,** 254–267.

Ito T, Takahashi N, Shimura Y, Okada K. 1997. A serine/threonine protein kinase gene isolated by an *in vivo* binding procedure using the Arabidopsis floral homeotic gene product, AGAMOUS. *Plant and Cell Physiology* **38,** 248–258.

Jack T. 2001. Plant development going MADS. *Plant Molecular Biology* **46,** 515–520.

Jones JDG, Dunsmuir P, Bedbrook J. 1985. High level expression of introduced chimeric genes in regenerated transformed plants. *The EMBO Journal* **4,** 2411–2418.

Kieber JJ, Rothenberg M, Roman G, Feldmann KA, Ecker JR. 1993. CTR1, a negative regulator of the ethylene response pathway in Arabidopsis, encodes a member of the raf family of protein kinases. *Cell* **72,** 427–441.

Kramer EM, Jaramillo MA, Di Stilio VS. 2004. Patterns of gene duplication and functional evolution during the diversification of the AGAMOUS subfamily of MADS box genes in angiosperms. *Genetics* **166,** 1011–1023.

Lee H-S, Chung Y-Y, Das C, Karunanandaa B, van Went JL, Mariani C, Kao T-H. 1997. Embryo sac development is affected in *Petunia inflata* plants transformed with an antisense gene encoding the extracellular domain of receptor kinase PRK1. *Sexual Plant Reproduction* **10,** 341–350.

Lee H-S, Karunanandaa B, McCubbin A, Gilroy S, Kao T-h. 1996. PRK1, a receptor-like kinase of *Petunia inflata*, is essential for postmeiotic development of pollen. *The Plant Journal* **9,** 613–624.

Li J, Chory J. 1997. A putative leucine-rich repeat receptor kinase involved in brassinosteroid signal transduction. *Cell* **90,** 929–938.

Liu Z, Franks RG, Klink VP. 2000. Regulation of gynoecium marginal tissue formation by LEUNIG and AINTEGUMENTA. *The Plant Cell* **12,** 1879–1892.

Liu Z, Meyerowitz EM. 1995. LEUNIG regulates AGAMOUS expression in Arabidopsis flowers. *Development* **121,** 975–991.

Lorbiecke R, Steffens M, Tomm JM, Scholten S, von Wiegen P, Kranz E, Wienand U, Sauter M. 2005. Phytosulphokine gene regulation during maize (*Zea mays* L.) reproduction. *Journal of Experimental Botany* **56,** 1805–1819.

Lukowitz W, Roeder A, Parmenter D, Somerville C. 2004. A MAPKK kinase gene regulates extra-embryonic cell fate in Arabidopsis. *Cell* **116,** 109–119.

Madhani HD, Fink GR. 1998. The riddle of MAP kinase signaling specificity. *Trends in Genetics* **14,** 151–155.

Mandel MA, Bowman JL, Kempin SA, Ma H, Meyerowitz EM, Yanofsky MF. 1992. Manipulation of flower structure in transgenic tobacco. *Cell* **71,** 133–143.

Matsubayashi Y, Ogawa M, Morita A, Sakagami Y. 2002. An LRR receptor kinase involved in perception of a peptide plant hormone, phytosulfokine. *Science* **296,** 1470–1472.

Matton DP, Maes O, Laublin G, Xike Q, Bertrand C, Morse D, Cappadocia M. 1997. Hypervariable domains of self-incompatibility

RNases mediate allele-specific pollen recognition. *The Plant Cell* **9,** 1757–1766.

Modrusan Z, Reiser L, Feldmann KA, Fischer RL, Haughn GW. 1994. Homeotic transformation of ovules into carpel-like structures in Arabidopsis. *The Plant Cell* **6,** 333–349.

Murphy LO, Blenis J. 2006. MAPK signal specificity: the right place at the right time. *Trends in Biochemical Science* **31,** 268–275.

Nadeau JA, Sack FD. 2002. Control of stomatal distribution on the Arabidopsis leaf surface. *Science* **296,** 1697–1700.

Nishihama R, Banno H, Shibata W, Hirano K, Nakashima M, Usami S, Machida Y. 1995. Plant homologues of components of MAPK (mitogen-activated protein kinase) signal pathways in yeast and animal cells. *Plant and Cell Physiology* **36,** 749–757.

O'Brien M, Bertrand C, Matton DP. 2002*a*. Characterization of a fertilization-induced and developmentally regulated plasma-membrane aquaporin expressed in reproductive tissues, in the wild potato *Solanum chacoense* Bitt. *Planta* **215,** 485–493.

O'Brien M, Chantha SC, Rahier A, Matton DP. 2005. Lipid signaling in plants. cloning and expression analysis of the obtusifoliol 14α-demethylase from *Solanum chacoense* Bitt., a pollination- and fertilization-induced gene with both obtusifoliol and lanosterol demethylase activity. *Plant Physiology* **139,** 734–749.

O'Brien M, Kapfer C, Major G, Laurin M, Bertrand C, Kondo K, Kowyama Y, Matton DP. 2002*b*. Molecular analysis of the stylar-expressed *Solanum chacoense* small asparagine-rich protein family related to the HT modifier of gametophytic self-incompatibility in *Nicotiana*. *The Plant Journal* **32,** 985–996.

O'Brien M, Gray-Mitsumune M, Kapfer C, Bertrand C, Matton DP. 2006. The ScFRK2 MAP kinase kinase kinase from *Solanum chacoense* affects pollen development and viability. *Planta* (in press).

Pinyopich A, Ditta GS, Savidge B, Liljegren SJ, Baumann E, Wisman E, Yanofsky MF. 2003. Assessing the redundancy of MADS-box genes during carpel and ovule development. *Nature* **424,** 85–88.

Piwien-Pilipuk G, Huo JS, Schwartz J. 2002. Growth hormone signal transduction. *Journal of Pediatric Endocrinology and Metabolism* **15,** 771–786.

Posas F, Saito H. 1997. Osmotic activation of the HOG MAPK pathway via Ste11p MAPKKK: scaffold role of Pbs2p MAPKK. *Science* **276,** 1702–1705.

Ray A, Robinson-Beers K, Ray S, Baker SC, Lang JD, Preuss D, Milligan SB, Gasser CS. 1994. Arabidopsis floral homeotic gene BELL (BEL1) controls ovule development through negative regulation of AGAMOUS gene (AG). *Proceedings of the National Academy of Sciences, USA* **91,** 5761–5765.

Robinson MJ, Cobb MH. 1997. Mitogen-activated protein kinase pathways. *Current Opinion in Cell Biology* **9,** 180–186.

Romeis T. 2001. Protein kinases in the plant defence response. *Current Opinion in Plant Biology* **4,** 407–414.

Saitou N, Nei M. 1987. The Neighbor–Joining method: a new method for reconstructing phylogenetic trees. *Molecular Biology and Evolution* **4,** 406–425.

Sambrook J, Fritsch EF, Maniatis T. 1989. *Molecular cloning: a laboratory manual*. Cold Spring Harbor, NY: Cold Spring Harbor Laboratory Press.

Samuel MA, Ellis BE. 2002. Double jeopardy: both overexpression and suppression of a redox-activated plant mitogen-activated protein kinase render tobacco plants ozone sensitive. *The Plant Cell* **14,** 2059–2069.

Schmidt ED, Guzzo F, Toonen MA, de Vries SC. 1997. A leucine-rich repeat containing receptor-like kinase marks somatic plant cells competent to form embryos. *Development* **124,** 2049–2062.

Schneitz K, Hulskamp M, Kopczak SD, Pruitt RE. 1997. Dissection of sexual organ ontogenesis: a genetic analysis of ovule development in *Arabidopsis thaliana*. *Development* **124,** 1367–1376.

Sells MA, Knaus UG, Bagrodia S, Ambrose DM, Bokoch GM, Chernoff J. 1997. Human p21-activated kinase (Pak1) regulates actin organization in mammalian cells. *Current Biology* **7,** 202–210.

Sugden PH, Clerk A. 1997. Regulation of the ERK subgroup of MAP kinase cascades through G protein-coupled receptors. *Cell Signaling* **9,** 337–351.

Tanaka H, Watanabe M, Watanabe D, Tanaka T, Machida C, Machida Y. 2002. *ACR4*, a putative receptor kinase gene of *Arabidopsis thaliana*, that is expressed in the outer cell layers of embryos and plants, is involved in proper embryogenesis. *Plant and Cell Physiology* **43,** 419–428.

Thompson JD, Gibson TJ, Plewniak F, Jeanmougin F, Higgins DG. 1997. The CLUSTAL_X windows interface: flexible strategies for multiple sequence alignment aided by quality analysis tools. *Nucleic Acids Research* **25,** 4876–4882.

Tieman DM, Ciardi JA, Taylor MG, Klee HJ. 2001. Members of the tomato *LeEIL* (*EIN3-like*) gene family are functionally redundant and regulate ethylene responses throughout plant development. *The Plant Journal* **26,** 47–58.

Tonaco IA, Borst JW, de Vries SC, Angenent GC, Immink RG. 2006. *In vivo* imaging of MADS-box transcription factor interactions. *Journal of Experimental Botany* **57,** 33–42.

Treisman R. 1996. Regulation of transcription by MAP kinase cascades. *Current Opinion in Cell Biology* **8,** 205–215.

Tu H, Barr M, Dong DL, Wigler M. 1997. Multiple regulatory domains on the Byr2 protein kinase. *Molecular and Cellular Biology* **17,** 5876–5887.

Vandenbussche M, Zethof J, Souer E, Koes R, Tornielli GB, Pezzotti M, Ferrario S, Angenent GC, Gerats T. 2003. Toward the analysis of the petunia MADS box gene family by reverse and forward transposon insertion mutagenesis approaches: B, C, and D floral organ identity functions require SEPALLATA-like MADS box genes in petunia. *The Plant Cell* **15,** 2680–2693.

Whelan S, Goldman N. 2001. A general empirical model of protein evolution derived from multiple protein families using a maximum-likelihood approach. *Molecular Biology and Evolution* **18,** 691–699.

Wilkinson J, Twell D, Lindsey K. 1997. Activities of CaMV 35S and nos promoters in pollen: implications for field release of transgenic plants. *Journal of Experimental Botany* **48,** 265–275.

Wu C, Leberer E, Thomas DY, Whiteway M. 1999. Functional characterization of the interaction of Ste50p with Ste11p MAPKKK in *Saccharomyces cerevisiae*. *Molecular Biology of the Cell* **10,** 2425–2440.

Zhang S, Klessig DF. 2001. MAPK cascades in plant defense signaling. *Trends in Plant Science* **6,** 520–527.